


## RESEARCH ARTICLE

# The implications of permafrost thaw and land cover change on snow water equivalent accumulation, melt and runoff in discontinuous permafrost peatlands

Ryan F. Connon<sup>1</sup>  | Laura Chasmer<sup>2</sup> | Emily Haughton<sup>3,4</sup> | Manuel Helbig<sup>5,6</sup> | Chris Hopkinson<sup>2</sup> | Oliver Sonnentag<sup>5</sup> | William L. Quinton<sup>3</sup>

<sup>1</sup>Environment and Natural Resources, Government of the Northwest Territories, Yellowknife, Northwest Territories, Canada

<sup>2</sup>Department of Geography and Environment, University of Lethbridge, Lethbridge, Alberta, Canada

<sup>3</sup>Cold Regions Research Centre, Wilfrid Laurier University, Waterloo, Ontario, Canada

<sup>4</sup>Hakai Institute, Campbell River, British Columbia, Canada

<sup>5</sup>Département de géographie & Centre d'études nordiques, Université de Montréal, Montréal, Quebec, Canada

<sup>6</sup>Department of Physics and Atmospheric Science, Dalhousie University, Halifax, Nova Scotia, Canada

## Correspondence

Ryan F. Connon, Department of Environment and Natural Resources, Government of the Northwest Territories, P.O. Box 1320, Yellowknife, NT X1A 2L9, Canada.  
Email: ryan\_connon@gov.nt.ca

## Funding information

ArcticNet; Natural Sciences and Engineering Research Council of Canada; Garfield Weston Foundation

## Abstract

In the discontinuous permafrost zone of the Northwest Territories (NWT), Canada, snow covers the ground surface for half the year. Snowmelt constitutes a primary source of moisture supply for the short growing season and strongly influences stream hydrographs. Permafrost thaw has changed the landscape by increasing the proportional coverage of permafrost-free wetlands at the expense of permafrost-cored peat plateau forests. The biophysical characteristics of each feature affect snow water equivalent (SWE) accumulation and melt rates. In headwater streams in the southern Dehcho region of the NWT, snowmelt runoff has significantly increased over the past 50 years, despite no significant change in annual SWE. At the Fort Simpson A climate station, we found that SWE measurements made by Environment and Climate Change Canada using a Nipher precipitation gauge were more accurate than the Adjusted and Homogenized Canadian Climate Dataset which was derived from snow depth measurements. Here, we: (a) provide 13 years of snow survey data to demonstrate differences in end-of-season SWE between wetlands and plateau forests; (b) provide ablation stake and radiation measurements to document differences in snow melt patterns among wetlands, plateau forests, and upland forests; and (c) evaluate the potential impact of permafrost-thaw induced wetland expansion on SWE accumulation, melt, and runoff. We found that plateaus retain significantly ( $p < 0.01$ ) more SWE than wetlands. However, the differences are too small (123 mm and 111 mm, respectively) to cause any substantial change in basin SWE. During the snowmelt period in 2015, wetlands were the first feature to become snow-free in mid-April, followed by plateau forests (7 days after wetlands) and upland forests (18 days after wetlands). A transition to a higher percentage cover of wetlands may lead to more rapid snowmelt and provide a more hydrologically-connected landscape, a plausible mechanism driving the observed increase in spring freshet runoff.

## KEYWORDS

land cover change, permafrost thaw, runoff, snow, snowmelt

## 1 | INTRODUCTION

Northwestern Canada is one of the most rapidly warming regions on Earth (Box et al., 2019; Vincent et al., 2015). It is expected that continued warming will exert considerable influence on snow accumulation, redistribution and melt patterns. These changes may result in a greater frequency of mid-winter snowmelt and rain-on-snow events (Putkonen et al., 2009), a shorter snow-covered season (Pachauri & Reisinger, 2007; Semmens et al., 2013), and greater inter-annual variability in snow depth (Hinzman et al., 2005). Such changes to the snow cover of this region have coincided with climate warming-induced permafrost thaw (Goodrich, 1982; Quinton et al., 2011), and the resulting changes to active layer (i.e., seasonally frozen and thawed) properties (Connon et al., 2018) and ecosystem composition, structure and function (Helbig, Wischniewski, et al., 2016; Jorgenson et al., 2001; Pulliainen et al., 2017). The combined effects of such changes to snow, permafrost, and ecosystems on water storage and flow processes are poorly understood, and as a result, there is considerable uncertainty regarding the long-term impact of climate change on the water resources of this region.

The greatest rates of areal permafrost thaw in northwestern Canada are found near the southern limit of discontinuous permafrost (Helbig, Pappas, & Sonnentag, 2016b), where permafrost exists primarily in low-lying, peatland-dominated areas (Kwong & Gan, 1994; Robinson & Moore, 2000). The permafrost of this region is highly susceptible to thaw because it is spatially fragmented, and as such, receives heat conducted laterally from non-permafrost bodies (Devoie et al., 2019) in addition to heat conducted vertically from the ground surface (Chasmer et al., 2011; Kurylyk et al., 2016). Moreover, because the permafrost of this region is thin (<10 m) and at the freezing temperature, little energy is required to initiate thaw (Quinton et al., 2009).

In the peatland-dominated lowlands of northwestern Canada, permafrost persists beneath forested peat plateaus that rise 1–2 m above permafrost-free, collapse scar wetlands developed from thermokarst erosion of the plateaus (Jorgenson & Osterkamp, 2005; NWWG, 1988). Although collapse scar wetlands are typically treeless (Zoltai, 1993), recent findings have suggested that permafrost thaw-induced partial drainage of such wetlands enables re-establishment of black spruce (*Picea mariana*) patches in the absence of permafrost (Disher et al., 2021; Haynes et al., 2018).

In response to climate warming, the permafrost below peat plateaus is rapidly thawing, thereby changing the proportion of landscape covered by peat plateaus to that occupied by collapse scar wetlands (Quinton et al., 2003). Tree mortality is especially pronounced along the edges of peat plateaus where permafrost thaw has caused the ground surface to subside and rooting networks to become inundated (Chasmer et al., 2011; Zoltai, 1993). This process, which occurs in boreal peat landscapes with discontinuous permafrost, is increasing the areal coverage of wetlands at the expense of plateaus (Quinton et al., 2011; Robinson & Moore, 2000; Thie, 1974). Given the differences in snow accumulation rates between forests and open environments (Sicart et al., 2004), plateau to wetland land cover change could

impact basin snow distribution and melt regimes, and also, flux and storage of snowmelt water.

In the permafrost-free, central boreal forest region of Canada, the structure of the canopy and canopy openings can have a significant influence on the distribution of snow and snow water equivalent (SWE). For example, Pomeroy and Schmidt (1993) found that a boreal black spruce canopy in central Saskatchewan intercepted 60% of cumulative snowfall and lost over 30% of annual snowfall to sublimation from canopy interception. Storck et al. (2002) found a similar rate of canopy interception in a montane environment, while others (e.g., Maxwell & St Clair, 2019) found that tree canopy removal led to substantial increases of SWE on the ground because of reduced interception and sublimation. Spatial and seasonal snow depth observations in montane regions indicate snow accumulation is greatest within the forest ecotone between open and closed canopies, where snow redistributed from openings can accumulate (e.g., Cartwright et al., 2020; Hiemstra et al., 2002). The SWE accumulated in this type of ecotone therefore depends on the perimeter and the edge to area ratio of the opening. The fractional canopy cover of more northern, forested permafrost peatlands is lower than at permafrost-free sites of the southern and central boreal region, suggesting that canopy interception and sublimation would also be lower. However, end-of-winter SWE of peat plateaus and adjacent wetlands in the sporadic to discontinuous permafrost zone have not been evaluated. We hypothesize that conversion of forest to wetland resulting from thermokarst processes has the potential to alter the total SWE in a basin by the end-of-winter.

In northern environments, the spring freshet typically releases about half the total annual precipitation within a relatively short period. This release occurs at a time when infiltration can be restricted by frozen ground (Gray et al., 2001) and when the runoff producing area (i.e., the effective basin area) is at or near its maximum spatial extent (Hayashi et al., 2004; Roulet & Woo, 1986). Changes to snow accumulation and melt regimes in combination with land cover changes that increase hydrological connectivity have the potential to alter the hydrograph response of streams and rivers in northwestern Canada. Permafrost thaw has increased the hydrological connectivity of peatland-dominated terrains, and as a result, drainage basins occupying such terrains route water from their land covers to their drainage networks with increasing efficiency (Connon et al., 2015; Haynes et al., 2018) and therefore produce greater basin discharge (Chasmer & Hopkinson, 2016). By converting forests to wetlands, permafrost thaw therefore has the potential to affect both the spatial distribution of snow and snowmelt runoff processes, with implications for the volume and timing of the basin discharge response. Using end-of-winter snow survey data, snowmelt and micrometeorological measurements, as well as hydrometric and climate data, this study seeks to improve the understanding of how permafrost thaw-induced land cover change affects end-of-winter snow storage and snowmelt runoff generation. This is accomplished by investigating: 1) possible trends in annual snowfall from long-term publicly available datasets in the southern Dehcho region of the Northwest Territories; 2) how end-of winter SWE accumulation and snowmelt rates vary between

forest and wetlands; and 3) how permafrost thaw-induced land cover changes may alter basin hydrographs.

## 2 | STUDY SITE

Scotty Creek ( $61^{\circ}18' \text{ N}$ ,  $121^{\circ}18' \text{ W}$ ), located within the Dehcho region of the Northwest Territories, Canada, drains a  $152 \text{ km}^2$  basin that lies approximately 50 km south of Fort Simpson (Figure 1). The Fort Simpson region has a dry continental climate with short, warm summers (average July temperature of  $17.5^{\circ}\text{C}$ ) and long, cold winters (average January temperature of  $-24.3^{\circ}\text{C}$ ). Daily average air temperature (1981–2010) recorded at the Environment and Climate Change Canada (ECCC) Fort Simpson A station is  $-2.6^{\circ}\text{C}$ . Fort Simpson receives an average of 390 mm of precipitation annually, of which 149 mm falls as snow. Snowmelt usually commences in mid-April and most snow has disappeared from the landscape by the end of April (Hamlin et al., 1998).

The Scotty Creek watershed contains upland forests (48%), wetlands (31%), peat plateaus (20%) and lakes (2%) (Chasmer et al., 2014). The reader is referred to Garon-Labrecque et al. (2016) for a detailed account of the vegetation communities at the study site. The headwater portion of the watershed is mantled by 2–8 m thick peat cover (McClymont et al., 2013) overlying a clay/silt-clay glacial till deposit of low permeability (Aylesworth & Kettles, 2000), and dominated by peat plateaus covered by black spruce forest underlain by permafrost; and treeless, permafrost-free wetlands, predominantly collapse scars and channel fens. The peat plateaus and collapse scars collectively form plateau-wetland complexes separated by channel fens. Within the plateau-wetland complexes, collapse scar wetlands include relatively small, circular features, indicating relatively recent formation; and larger (>100 m diameter) thermokarst features with more complex shapes resulting from the merger of wetlands following the thaw of intervening permafrost (Quinton et al., 2011). Variations in the size and shape of wetlands and intervening plateaus influence the spatial variations of processes such as canopy interception of snowfall

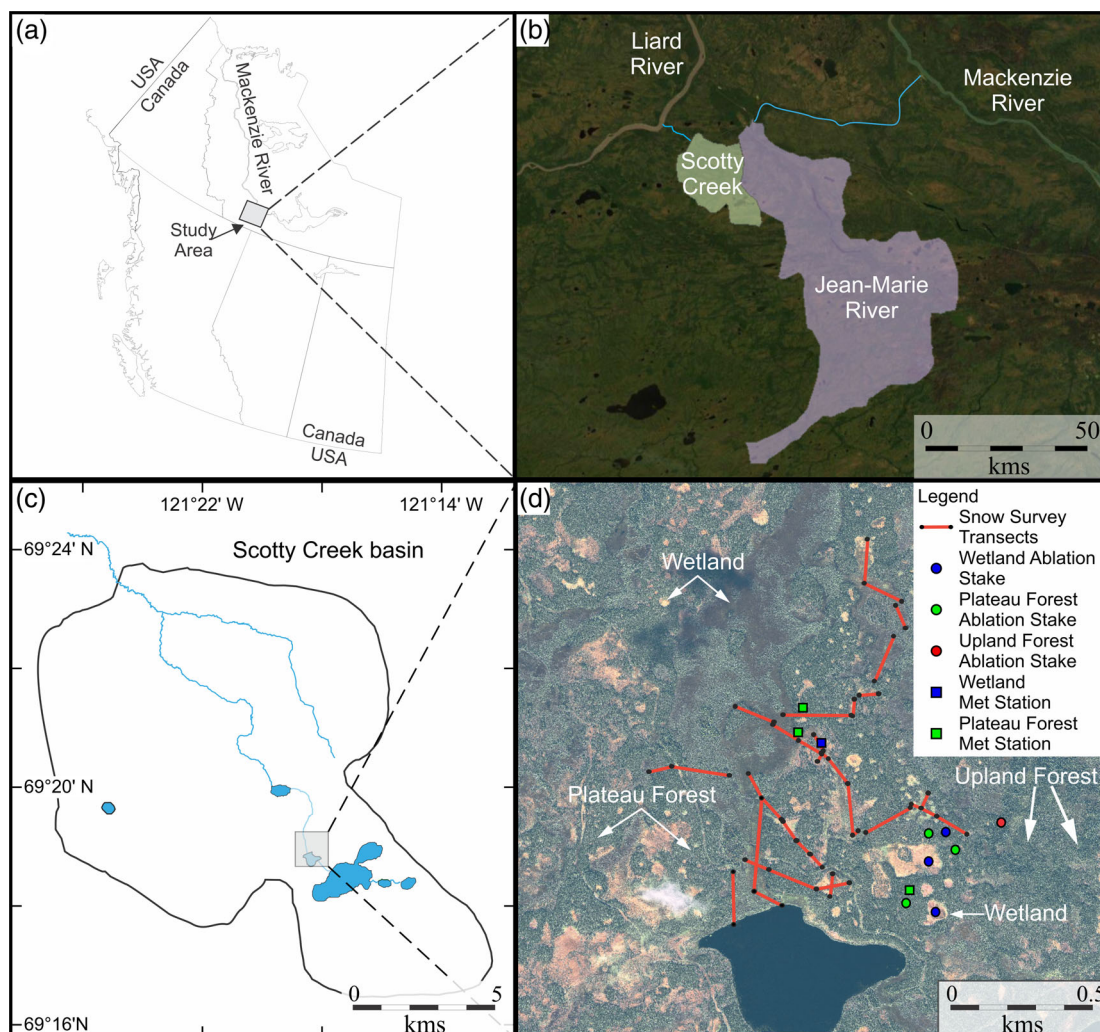


**FIGURE 1** The locations of the (a) study region within the Northwest Territories, Canada; (b) Scotty Creek and Jean Marie River drainage basins upstream of the water survey of Canada gauging stations, with channel sections downstream of the gauging stations indicated by in light blue; (c) the Scotty Creek drainage basin, and within it, the area used for field studies in the current study; and (d) a 2018 WorldView 3 image of the study area identifying the major land cover types and locations where measurements were taken

(e.g., Storck et al., 2002) and vegetation trapping of blowing snow (e.g., Cartwright et al., 2020). As a result, the depth of snow accumulation also varies across the landscape.

### 3 | METHODS

#### 3.1 | Trends in annual snowfall

The shorter-term in-situ SWE data record at Scotty Creek (2006–2020) was not long enough to determine if there has been a significant long-term change in SWE accumulation over the southern Dehcho region matching the length of finalized hydrometric records (1972–2017). However, SWE observations have been conducted by Environment and Climate Change Canada at the Fort Simpson Airport since 1896. To determine if SWE values collected at Fort Simpson could provide a reasonable estimation as to whether there has been a statistically significant change in SWE at Scotty Creek, SWE values were compared for the common period of record at both locations (2006–2018, with the exception of 2008). SWE data from Scotty Creek were collected using annual snow surveys and SWE from Fort Simpson was reported and analysed from two different ECCC sources: 1) the Adjusted and Homogenized Canadian Climate Data (AHCCD) (Mekis & Vincent, 2011); and 2) non-adjusted data from the Fort Simpson A weather station (station IDs: 1656 and 52 780). When comparing data from Fort Simpson and Scotty Creek, cumulative Fort Simpson SWE was calculated from the onset of snowfall until the final day of snow surveys during that field campaign, which typically fell within the last 2 weeks of March. All water flux values are reported for the water year (01 October –30 September).

ECCC publishes the AHCCD for hundreds of surface weather stations across Canada (Mekis & Vincent, 2011); including the weather station at Fort Simpson Airport. For the purposes of the AHCCD, ECCC uses their station measurements of snow depth to derive SWE values as follows:

$$SWE = d_s * \rho_s * SWE_{adj}$$

where  $d_s$  is snow depth measured using a snowfall ruler,  $\rho_s$  is the density of fresh snowfall (assumed to be  $100 \text{ kg m}^{-3}$ ), and  $SWE_{adj}$  is a location-specific SWE adjustment factor (Mekis & Brown, 2010; Mekis & Hopkinson, 2004; Mekis & Vincent, 2011). During the 1990s, a station modernization program introduced automated snow depth measurements using SR50 and SR50A (Campbell Scientific, Logan, UT) ultrasonic snow depth sensors (Mekis et al., 2018). Publicly available metadata that outlines measurement techniques and instruments is under development (Mekis et al., 2018), so it was not possible to determine the exact date of the introduction of automated snow depth measurements. However, based on the deviation of the close relationship between SWE derived from snow depth and SWE measured in an adjacent Nipher precipitation gauge (Figure 2(a)), it appears that snow depth measurements at the Fort Simpson A station transitioned from manual (snow ruler) to automatic (Campbell Scientific's SR50 and SR50A) in 1994.

Manual Canadian Nipher gauges were introduced by ECCC in the 1960s for winter snowfall measurements (Mekis et al., 2018). Based on non-adjusted, publicly available ECCC data, the 'total precipitation (mm)' field was populated by Nipher gauge data beginning in February, 1964. Prior to this, the 'total precipitation (mm)' and 'snow depth (cm)' fields contained identical values, which implies that an assumed snow density of  $100 \text{ kg m}^{-3}$  was applied to snow ruler depth measurements to obtain a precipitation value in mm. From February 1964 onwards, the values in the 'total precipitation (mm)' and 'snow depth (cm)' fields were similar, but not identical, suggesting two independent measures. Although not corrected for undercatch, Goodison et al. (1998) report that Canadian Nipher gauges have high catch efficiency (>90% when wind speeds are  $<3 \text{ m s}^{-1}$ ), suggesting that the Nipher gauge measurements can provide a reasonable estimation of total SWE.

The non-adjusted SWE dataset was obtained from the ECCC 'Fort Simpson A' station. The data were ingested using the 'weathercan' package in the R statistical computing environment (R Core Team, 2013). Annual SWE was calculated as the sum of the total precipitation when daily average air temperatures were  $<0^\circ\text{C}$ .

#### 3.2 | SWE variability among land cover types

#### 3.3 | Snow surveys (2006–2020)

Snow surveys have been conducted at Scotty Creek every year near the end of March since 2006, with the exception of 2008 (no field personnel) and 2019 (an early March snowmelt event). There are 24 snow survey transects which span wetland and plateau forest land cover types of varying size (Figure 1(d)). Snow depth is measured at discrete points along each transect at ratios of between 5 and 10 depth measurements per density measurement, such that each transect has a minimum of five density measurements. Care was taken to ensure that measurements for both wetland and forest covers were not biased by overrepresentation of measurements taken at the edge of forest or wetland features, where transitional topography and vegetation structure (e.g., tilted trees) may impact snow accumulation and retention (Baltzer et al., 2014). Snow depth was measured using a wooden ruler, and snow density was measured using an Eastern Snow Conference (ESC) 30 snow tube ( $30 \text{ cm}^2$  cutting end cross sectional area; GeoScientific, Vancouver, BC, Canada) with a calibrated scale. Snow tubes with a cutting end cross sectional area of  $30 \text{ cm}^2$  show the lowest measurement error when used to sample snowpacks with a depth of less than 1 m (Kinar & Pomeroy, 2015). Published measurement errors of such snow tubes report a range of under-measurement of true SWE from 0.3% (Farnes et al., 1982; ESC-30 snow tube) to 9.7% (Dixon & Boon, 2012; Snow-Hydro snow tube, Fairbanks, AK). Under-measurement of SWE has been attributed to potential snow jamming in the snow tube due to internal stratification (Dixon & Boon, 2012).

For statistical analysis, snow survey data were aggregated into a land cover class of wetland or plateau. A filter was applied to the data



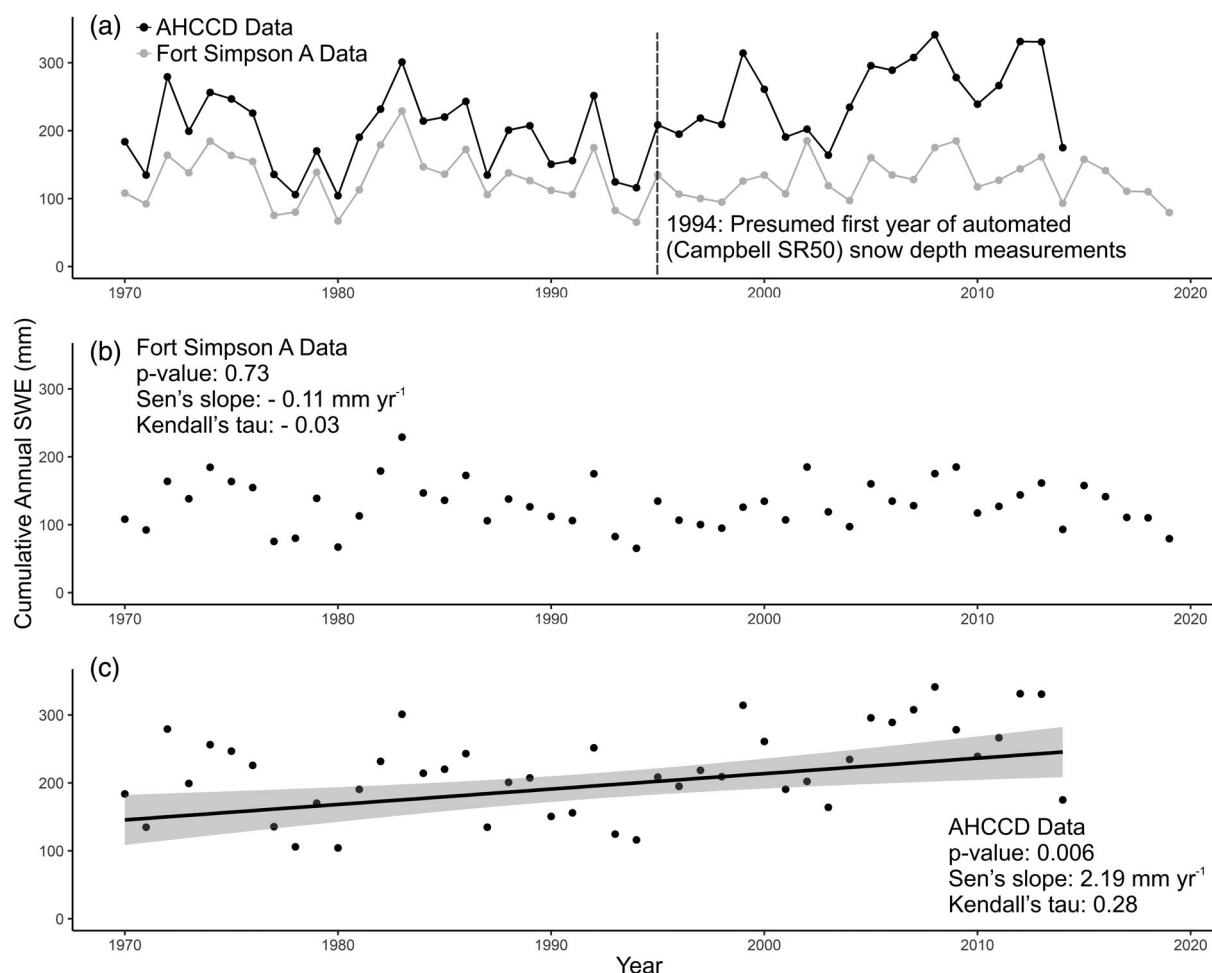


**FIGURE 2** (a) Comparison of annual (water year) Fort Simpson SWE values from the adjusted and homogenized Canadian climate dataset (AHCCD) and SWE derived from the Fort Simpson A weather station data from 1970 to 2014 (AHCCD) and 2019 (Fort Simpson A); (b) non-significant trend for SWE derived from Fort Simpson A weather station data; and (c) significant increasing trend for AHCCD SWE data

to only include snow density values ranging from two standard deviations below the mean value and three standard deviations above the mean value. The lower bound was less than the higher bound to ensure that the minimum density was still higher than the generally accepted density of fresh snow ( $0.1 \text{ kg m}^{-3}$ ; Mekis & Vincent, 2011). This yielded a range of densities from  $0.11 \text{ g cm}^{-3}$  to  $0.29 \text{ g cm}^{-3}$  and retained over 97% of the original data, while allowing for the removal of possible measurement (e.g., snow falling from the tube before measurement) or data entry errors.

### 3.4 | Snowmelt measurements (2015)

Intensive snowmelt measurements were collected in April and May 2015. Measurements were typically collected at least every other day using ablation stakes at three wetland sites, three plateau forest sites, and an upland forest site (Figure 1(d)). Each ablation stake consisted of a 2.0 m long taught wire, installed 1.2 m above the ground, extending over the snow surface between two steel rods embedded in the frozen ground. Ablation at each stake was derived from the average vertical displacement of the snowpack surface below 11 evenly-spaced points

along the wire over a period of between 24 and 48 h. Depth-integrated snow samples were measured from a snow pit adjacent to each stake, although at a sufficient distance so as not to affect the snowpack below the stake. A  $100 \text{ cm}^3$  snow sample taken from each distinct layer was weighed with an electronic scale (Light Duty Crane Scale; BC Scale, Langley, BC, Canada), and a mean snowpack density was computed. This allowed the average vertical displacement measured at each stake to be expressed in terms of SWE. The differences in average SWE between successive measurements provided the snowmelt rate over the intervening time period.

### 3.5 | Micrometeorological measurements

The four components of net radiation (incoming and outgoing short-wave and longwave) were measured at four locations during the snowmelt period in 2015, including three on forested plateaus and one in a wetland (Figure 1(d)). Collectively, the three plateau sites are representative of the variation in tree canopy density found within the watershed (sparse, average and dense) and therefore, the sub-canopy variation of radiation regimes (Webster et al., 2016).

Sub-canopy radiation was measured using four component net radiometers (CNR1, Kipp and Zonen, Delft, the Netherlands) connected to data loggers (CR 1000, Campbell Scientific, Logan, UT), which measured a sample every minute, and averaged and recorded values every 30 minutes. The radiometers were installed between 1.45 m and 2.00 m above the ground surface, resulting in sub-canopy radiation measurements on plateaus and open measurements in the wetland. At the time of snowmelt at the end of winter, these sensors were approximately 0.65 to 1.20 m above the snow surface, and as such, the upward-directed fluxes they measured were assumed to be radiation reflected or emitted from the underlying snow surface. Unfortunately longwave radiation data were not available at the average plateau forest location in 2015 due to power issues. A complete description of micrometeorological instrumentation design can be found in Haynes et al. (2019).

### 3.6 | Permafrost thaw-induced hydrological change

The Water Survey of Canada installed a hydrometric gauge near the outlet of Scotty Creek in 1995 and has monitored basin discharge continually since then. A longer-term hydrometric record (1972–2017) is also available from the Water Survey Canada for the adjacent 1310 km<sup>2</sup> Jean-Marie River basin, which was used to calculate trends over time. The data were ingested using the ‘tidyhydat’ package in the R statistical computing environment (R Core Team, 2013). Because the Jean-Marie River basin is similar to the Scotty Creek basin in terms of land cover types and proportions, the density and average slope of its channel network (Quinton et al., 2003), and its hydrological response (Chasmer & Hopkinson, 2016), it was used as a proxy for Scotty Creek runoff given the longer data record.

### 3.7 | Statistical analysis

All statistical analysis was completed using R (R Core Team, 2013). Time series analyses for changes to annual runoff and precipitation were calculated using the non-parametric Mann-Kendall test (Kendall, 1975) and were tested for autocorrelation. Slopes were calculated using the Kendall Thiel robust line (Helsel & Hirsch, 2002). The Kruskal–Wallis test was used to determine if there were statistically significant differences between datasets (Helsel & Hirsch, 2002; Kruskal & Wallis, 1952).

## 4 | RESULTS

### 4.1 | Trends in annual snowfall

The two ECCC SWE datasets from Fort Simpson yielded large differences in annual cumulative SWE, suggesting discrepancies in the way data were derived. After 1994, when AHCCD SWE values were derived from automated snow depth data instead of manual snow

ruler data, the median annual cumulative SWE from the AHCCD was 239 mm and the interquartile range (IQR) was 94 mm, whereas the median annual cumulative SWE from the Fort Simpson A data over the same period was 127 mm (IQR = 37 mm). The median SWE value from the entire 13-year Scotty Creek snow survey record was 120 mm (IQR = 36 mm), which more closely resembles the SWE values from the Fort Simpson A data than the AHCCD data. For comparison, the Department of Environment and Natural Resources of the Government of the Northwest Territories also completes annual snow surveys near Fort Simpson. The median SWE value for these snow surveys is 103 mm (IQR = 28 mm) for a data record that spans 1983–2000 and from 2013 to 2021. Although these snow surveys are completed in different land cover types and with slightly different methodologies than the Scotty Creek snow surveys, it provides evidence that the Fort Simpson A dataset produces more realistic values of cumulative annual SWE than the AHCCD.

The SWE values obtained from the AHCCD and the Fort Simpson A dataset also produce differences in trends. The high values for the period 1994 to 2014 in the AHCCD generate a significant increasing trend ( $p < 0.05$ ) of 0.11 mm yr<sup>-1</sup> in SWE for the period 1970–2014. There is no statistically significant trend in the Fort Simpson A dataset (Figure 2) for the same period ( $p > 0.05$ ). Based on this analysis, we suggest that the AHCCD SWE values overestimate actual SWE beginning in 1994 and therefore falsely suggest an increasing trend of cumulative annual SWE in Fort Simpson.

For the common 12 year period when both Fort Simpson A SWE data and Scotty Creek snow survey SWE data are available (Figure 3), the median annual SWE at Fort Simpson was 120 mm (IQR = 36 mm) and the median annual SWE at Scotty Creek was 124 mm (IQR = 40 mm). Although the total annual SWE was derived from snow surveys at Scotty Creek and was calculated as cumulative daily SWE at Fort Simpson, there was no statistically significant difference between the datasets ( $p > 0.05$ ), suggesting that the Fort Simpson A annual cumulative SWE data are a reasonable proxy for Scotty Creek SWE data for years when snow survey measurements are not available. Given that there is no statistically significant change in cumulative annual SWE at the Fort Simpson A gauge, we suggest that there is no statistically significant change in annual SWE in the Scotty Creek watershed between 1970 and 2019 (Figure 2).

### 4.2 | Variations of snow properties among land covers

Based on all data collected since 2006 (forest:  $n = 2285$  depths, 628 densities; wetland:  $n = 3892$  depths, 1141 densities), the median forest SWE (124 mm; IQR = 40 mm) and median wetland SWE (111 mm; IQR = 42 mm) were significantly different ( $p < 0.01$ ), although by only ~10% (Figure 4). Given that error estimates for the type of snow tube used here range from 0.3 to 9.7% (Dixon & Boon, 2012; Farnes et al., 1982), it is possible that these differences could be a result of uncertainty in measurement technique, although the large sample size of the dataset and the fact that error would

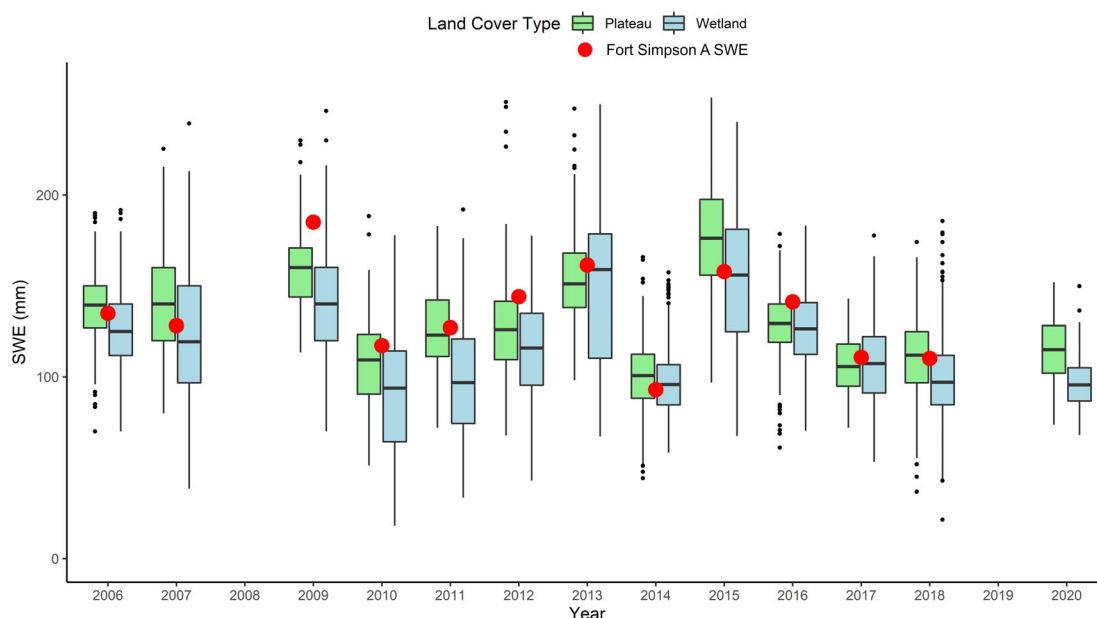


**FIGURE 3** Boxplots of SWE of plateau forests (green) and wetland (blue) ground surfaces measured at the end of each winter at Scotty Creek since 2006 on the snow survey transects indicated in Figure 1(d). The red circles indicate the sum of daily SWE measured at the Fort Simpson A weather station, where the calculation of annual SWE concludes on the same day that snow surveys at Scotty Creek were completed

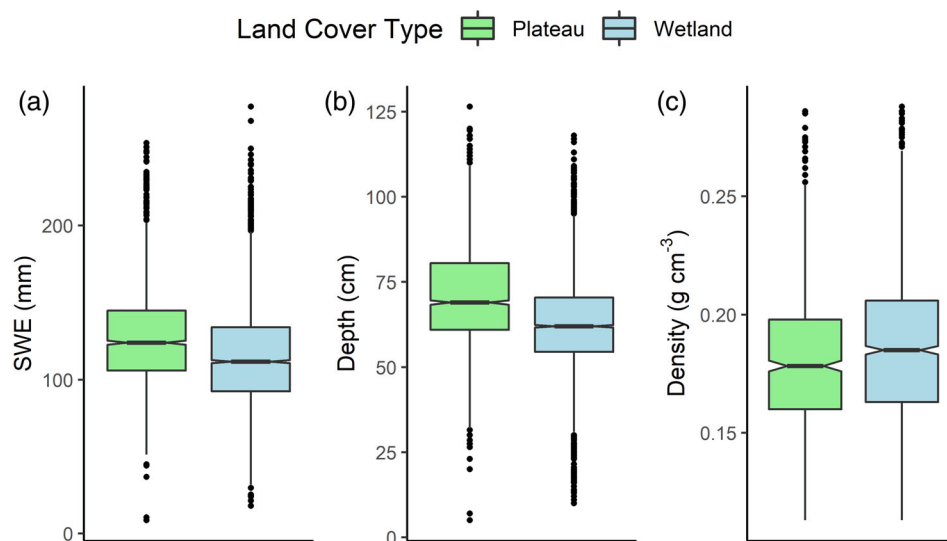


**FIGURE 4** Notched boxplots of (a) SWE, (b) snow depth and (c) snow density measured in plateau forests and wetlands from snow surveys at Scotty Creek. Values are derived from data from all years

occur independent of land cover type increases confidence in the difference presented here. The differences in SWE in each year were driven more by differences in snow depth than density. The median forest snow depth was 69 cm (IQR = 21 cm) and the median wetland depth was 62 cm (IQR = 15 cm), a difference that was statistically significant ( $p < 0.01$ ). The median forest density was  $0.178 \text{ g cm}^{-3}$  (IQR =  $0.040 \text{ g cm}^{-3}$ ) and the median wetland density was slightly higher at  $0.181 \text{ g cm}^{-3}$  (IQR =  $0.045 \text{ g cm}^{-3}$ ), a difference which was also statistically significant ( $p < 0.01$ ).

The SWE in forests was significantly higher ( $p < 0.01$ ) than wetlands in 10 of the 13 years. Snow depth in forests was significantly higher ( $p < 0.01$ ) than wetlands in 12 of the 13 years, while snow density was significantly higher ( $p < 0.01$ ) in wetlands in two of the 13 years, with the difference in density not being statistically

significant at the  $p < 0.01$  level for the remaining 11 years (Table 1). At the end of winter in 2015 (the year when snowmelt rates were measured), the median SWE of forests was 176 mm ( $n = 133$ ; IQR = 42 mm) and the median SWE of wetlands was 156 mm ( $n = 219$  depths; IQR = 56 mm) with a statistically significant ( $p < 0.01$ ) difference (Table 1).

### 4.3 | Variations of snowmelt rate among land covers

At the locations instrumented with ablation stakes in 2015 (Figure 1), initial SWE values prior to the onset of melt were relatively uniform for the wetland sites (125–144 mm;  $n = 3$ ) and more variable for the

**TABLE 1** Snow depth, density and SWE measured on the snow survey transects (Figure 1(d)) at Scotty Creek, and SWE measured at the Fort Simpson a gauge by environment and climate change Canada (ECCC) for the period 2006–2020. The sum of ECCC SWE data terminates on the final day that snow surveys were conducted in Scotty Creek of that year to provide accurate comparison

Year	Fort Simpson SWE (mm)	Scotty Creek									
		Land cover	Snow depth			Density			SWE		
			Sample (n)	Median (cm)	Different	Sample (n)	Median (g cm <sup>-3</sup> )	Different	Sample (n)	Median (mm)	Different
2006	118.2	Forest	203	74	***	97	0.189	***	203	139	***
		Wetland	424	65		208	0.196		424	125	
2007	121.6	Forest	144	79	***	70	0.182		144	140	***
		Wetland	243	65		118	0.188		244	119	
2008	162.5	No data at Scotty Creek this year due to lack of personnel									
2009	170.6	Forest	98	99	***	44	0.158		98	160	***
		Wetland	109	88		56	0.165		109	140	
2010	104.8	Forest	146	58	***	50	0.186	**	146	109	***
		Wetland	231	48		83	0.202		231	94	
2011	125.0	Forest	123	81	***	28	0.170	*	123	123	***
		Wetland	236	64		52	0.155		236	97	
2012	133.2	Forest	166	80	***	33	0.157	**	166	126	***
		Wetland	222	71		52	0.164		222	116	
2013	145.4	Forest	156	96	***	31	0.161		156	151	
		Wetland	227	92		50	0.172		227	159	
2014	89.4	Forest	215	59		38	0.175		215	101	***
		Wetland	441	59		100	0.165		441	96	
2015	154.6	Forest	133	80	***	30	0.223		133	176	***
		Wetland	219	67		53	0.233		219	156	
2016	114.6	Forest	309	65	***	64	0.201		309	129	**
		Wetland	492	64		114	0.200		492	126	
2017	109.4	Forest	167	67	***	39	0.157	***	167	106	
		Wetland	392	62		90	0.176		392	107	
2018	105.0	Forest	309	60	***	62	0.184	**	309	112	***
		Wetland	431	52		101	0.195		431	97	
2019	69.2	No data at Scotty Creek this year due to early snowmelt									
2020	No data	Forest	116	68	***	42	0.173	**	116	115	***
		Wetland	225	59		64	0.165		225	96	

Note: Asterisks denote the level of statistical significance (\* =  $p < 0.1$ , \*\* =  $p < 0.05$ , \*\*\* =  $p < 0.01$ ).

plateau forest sites (114–182 mm;  $n = 3$ ). The upland forest site had the highest initial SWE (184 mm). Snowmelt began at all sites on 07 April, while the rate of snowmelt at the wetland and plateau forest sites increased notably on 15 April (Figure 5). A similar increase at the upland forest site did not commence until 28 April. Snowmelt rates at the wetland sites were the most consistent and the most rapid. At the three instrumented sites, complete snow loss took between 13 and 14 days after the onset of melt. Snowmelt rates at the plateau forest sites were more variable as they took between 15 and 21 days to become snow free. Snowmelt at the upland forest did not conclude until 10 May, and lasted 33 days. The difference in melt rates can be attributed to different amounts of initial SWE, as well as differing canopy characteristics impacting energy available for snowmelt.

Table 2 provides mean daily radiation fluxes and albedo for three periods: 1) the period prior to the onset of snowmelt (28 March–06 April), the main snowmelt period for wetlands and plateau forests (07 April–28 April), and the initial post snowmelt period (29 April–10 May). Among the radiation flux components, incoming and outgoing shortwave radiation had the largest variability among sites (Figure 6). The correlation between snowmelt rate and incoming shortwave radiation was greater for the wetland ( $R^2 = 0.61$ ) than for the plateau forest ( $R^2 = 0.49$ ) (Figure 7). Prior to, and during snowmelt, the wetlands maintained a higher sub-canopy albedo than the plateau forests, but after snowmelt concluded, the sub-canopy albedo of wetlands decreased to a value similar to that of plateau forests (Figure 6(g)). Sub-canopy



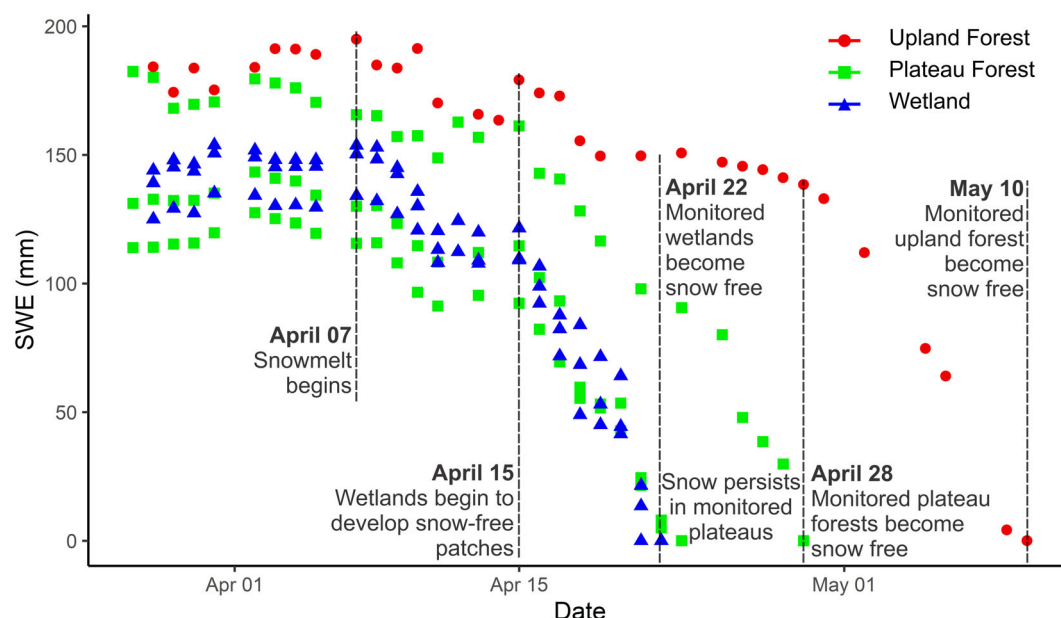


**FIGURE 5** Snowmelt rates at the end-of-winter in 2015 measured at three wetlands, three plateau forests, and a single location in the upland forest, as indicated in Figure 1(d)

**TABLE 2** Summary data for mean daily subcanopy radiation flux density parameters and albedo for the period prior to snowmelt (28 march–06 April), the snowmelt period (07 April–28 April), and the period after snowmelt concluded in the plateau forests and wetlands (29 April–10 may). Data are compiled for one wetland station and plateau forests of contrasting tree canopy density (sparse, average, and dense). Longwave radiation data were not available at the average plateau forest station during this time period

Variable	Before snowmelt				During snowmelt				After snowmelt			
	28 march–06 April				07 April–28 April				29 April–10 may			
	(MJ m <sup>-2</sup> d <sup>-1</sup> )				(MJ m <sup>-2</sup> d <sup>-1</sup> )				(MJ m <sup>-2</sup> d <sup>-1</sup> )			
	Wetland	Sparse	Average	Dense	Wetland	Sparse	Average	Dense	Wetland	Sparse	Average	Dense
Incoming shortwave	12.4	10.0	7.5	6.3	15.8	13.4	9.6	8.1	20.6	17.6	13.6	10.7
Incoming longwave	21.2	21.9		23.1	22.6	23.5		25.3	22.9	24.0		26.1
Outgoing shortwave	9.8	5.3	5.5	4.2	8.4	4.2	4.4	3.5	1.8	1.7	1.6	1.3
Outgoing longwave	24.0	24.5		24.7	26.4	27.0		27.1	29.4	29.9		29.7
Net shortwave	2.6	4.7	1.9	2.1	7.4	9.3	5.2	4.5	18.8	15.9	12.0	9.4
Net longwave	−2.8	−2.6		−1.6	−3.8	−3.6		−1.8	−6.5	−5.9		−3.5
Net radiation	−0.3	2.2		0.5	3.6	5.7		2.7	12.3	10.1		5.8
Albedo (unitless)	0.80	0.56	0.75	0.70	0.54	0.32	0.46	0.44	0.09	0.10	0.12	0.13

incoming longwave radiation was highest in the dense forest, and this flux increased as snowmelt progressed. Sub-canopy outgoing longwave radiation was constant among land cover features throughout the entire period. Total sub-canopy net radiation was initially highest in the sparse forest prior to and during snowmelt, but transitioned to being highest in the wetlands after they became snow-free.

#### 4.4 | Permafrost thaw-induced hydrological change

The median annual runoff from the Jean-Marie River for the period of record (1972–2017) was 111 mm (IQR = 81 mm), while the median

annual runoff from Scotty Creek for period of record (1995 to 2017) was 103 mm (IQR = 65 mm). There is a significant increasing trend ( $p < 0.05$ ) in annual streamflow over the period of record at Jean-Marie River.

Analysis of historical imagery of the Scotty Creek catchment indicated that between 1970 and 2015, the area occupied by peat plateau forest decreased from 55% to 40%, while wetland coverage increased from 36% to 51% (Chasmer & Hopkinson, 2016). The average annual loss of forest-covered terrain and concomitant annual increase in wetland area between 1970 and 2015 was 0.34% yr<sup>-1</sup> but increased to 0.58% yr<sup>-1</sup> between 2000 and 2015. Image analysis also demonstrated that forest loss / wetland expansion occurred preferentially along south facing edges of the plateaus (Chasmer & Hopkinson, 2016). These rates and patterns of land cover change are

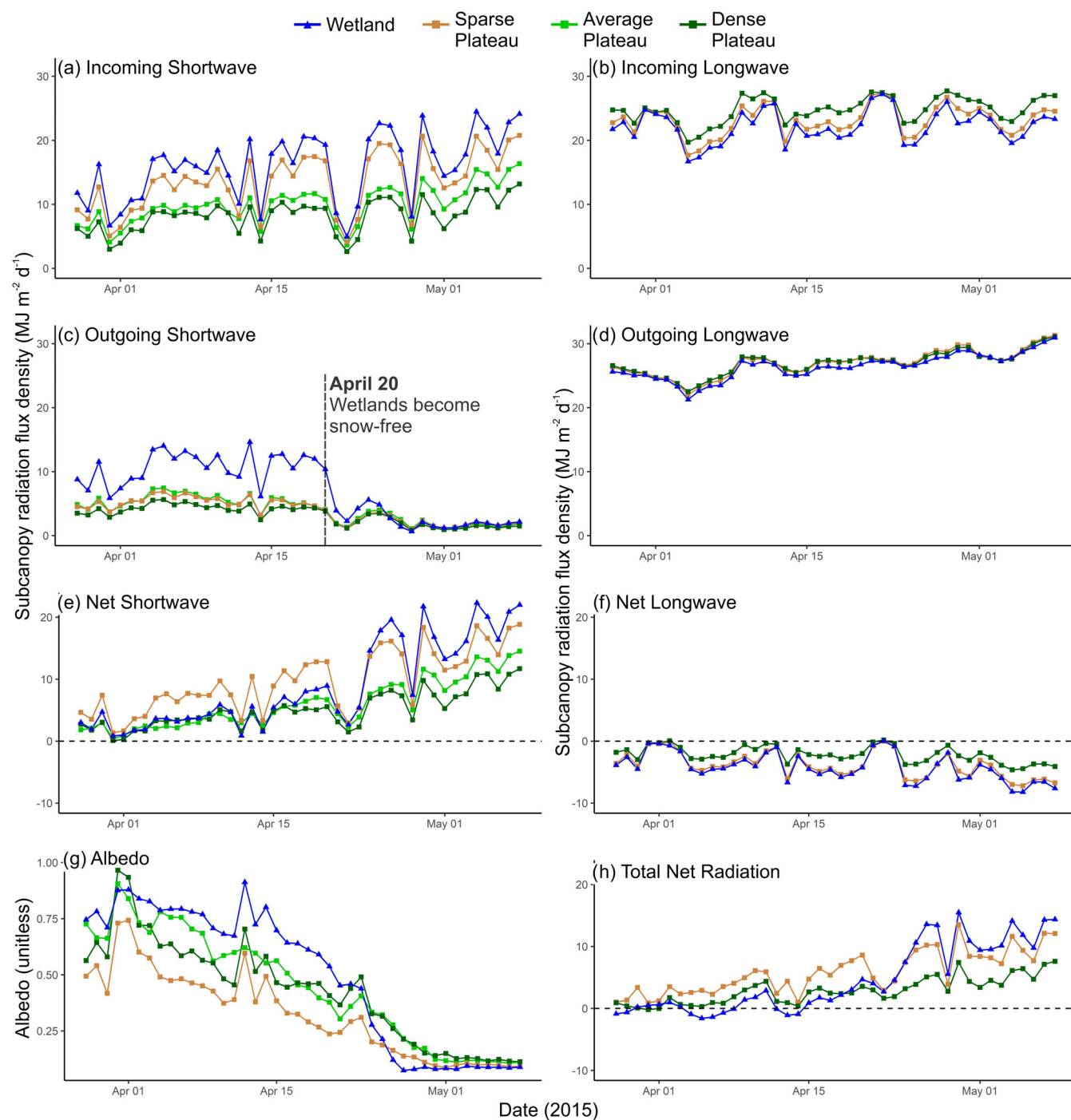


**FIGURE 6** Measurements of (a) incoming shortwave, (b) incoming longwave, (c) outgoing shortwave, (d) outgoing longwave, (e) net shortwave, (f) net longwave, (g) albedo and (h) total net radiation measured in 2015 at the stations located in a wetland and plateau forests of contrasting tree canopy density (sparse, average, and dense). Note that longwave radiation was not recorded at the average plateau due to sensor error

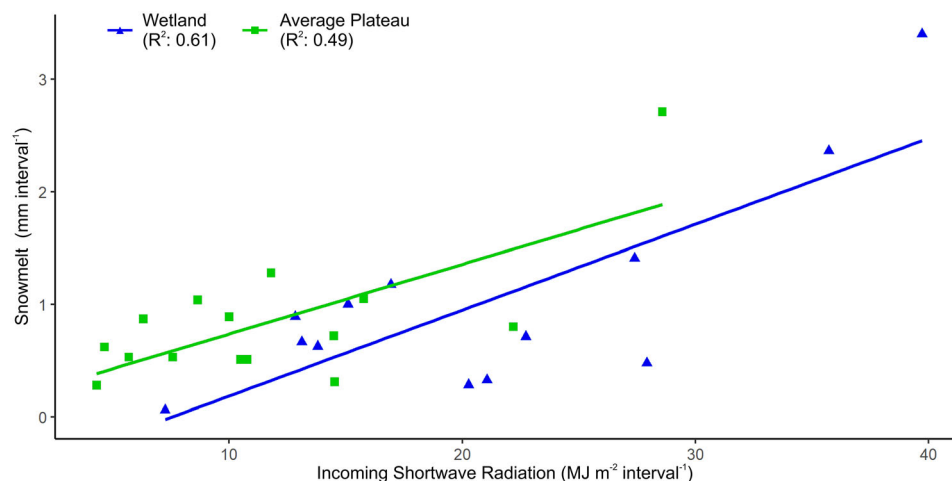
approximately consistent with those reported by Quinton et al. (2011), Connon et al. (2014), and Carpino et al. (2018). Using the median SWE values for plateau forests and wetlands and the land-cover change rates presented in Chasmer and Hopkinson (2016), the area-weighted SWE in the Scotty Creek basin decreased by less than 2% (117–115 mm) over the 45-year period as a result of permafrost thaw-induced conversion of forest to wetland.

## 5 | DISCUSSION

### 5.1 | Trends in annual snowfall

For the period of 1994–2014, we suggest that AHCCD overestimates the cumulative annual SWE at Fort Simpson. This overestimate is likely caused by inflated values of daily snowfall derived from the

**FIGURE 7** The average reduction in SWE between successive measurements at the ablation stakes of the plateau forests (green) and wetland (blue) sites plotted with the cumulative shortwave radiation measured over the same intervals. Measurement intervals ranged from 24 to 48 h



SR50A snow depth sensor. ECCC discontinued deriving snowfall measurements from SR50A sensors in December 2013 over concerns of wind effects and the unreliability of using single point measurements (Fischer, 2011; Mekis et al., 2018). The overestimation of snowfall between 1994 and 2014 was sufficiently large to erroneously indicate a trend of increasing SWE at Fort Simpson. Because of this, we suggest that care should be taken when assessing SWE trends at remote stations in northern Canada between the mid-1990s and 2014. Additional work across northern Canada is required to carefully determine the spatial extent of this overestimation.

## 5.2 | Variations of snow properties among land covers

The results presented here show higher SWE accumulations in forests relative to open wetlands contrary to results at more southern environments with higher fractional canopy coverage and/or more continuous canopy associated with commercial forest stands (Murray & Buttle, 2003; Winkler et al., 2005). In southern forests, the fractional canopy coverage is high enough to intercept appreciable quantities of snow. This increases sublimation of snow from the canopy and decreases snow accumulation on the ground (Varhola et al., 2010). In more northern forests, canopy interception is lower due to much lower canopy coverage. In this study, the higher SWE accumulation in forests is likely a result of the redistribution of SWE from the tree-less wetlands into the forest edges. Canopy interception in the forest plateaus is lower than in southern environments due to much lower canopy coverage in the former. For example, Golding and Swanson (1986) found that forest clearings with a fetch height of two to five times the height of adjacent trees will maximize SWE accumulation relative to forests because canopy interception and wind redistribution are both minimized. At Scotty Creek, the average canopy height ranges from ~3 to 6 m and canopy coverage ranges from 40% to 60% (Chasmer et al., 2011). Therefore, wetlands at Scotty Creek with a fetch length of between 6 and 30 m would retain the greatest SWE. The wetlands examined in this study all have fetch lengths that

exceed this threshold. Further work is needed to quantify SWE accumulation in smaller wetlands to determine if that threshold is maintained in the land covers studied here.

## 5.3 | Variations of snowmelt rate among land covers

The more rapid snowmelt rates in the wetlands than forests was expected since the open wetlands receive greater shortwave radiation input at the snow surface and lower longwave input because of the absence of longwave down-welling radiation from a canopy (e.g., Murray & Buttle, 2003; Varhola et al., 2010). This also suggests that net shortwave radiation is the primary source of energy available for snowmelt, which is consistent with other studies (e.g., Davis et al., 1996). Except for areas near the southern edge of wetlands where shading by trees can occur, the incoming shortwave radiation is homogeneous over wetland snow surfaces. By contrast, the spatial variability of the shortwave radiation flux over the forest snowpack is high as a result of variations of the overlying tree canopy. As a result, the spatial variation of melt is greater in the plateau forests than wetlands (Figure 5).

When wetlands began to develop snow-free patches around 15 April, melt rates increased dramatically (Figure 5). This acceleration of melt is likely a result of ponding water caused by: (1) restricted infiltration of meltwater due to near-surface ground ice; and (2) limited run-off from the wetland due to impoundment of drainage by permafrost. The ponding of near surface water and the stored energy associated with it would have contributed to the rapid melt of the remaining snowpack. Once the wetlands became snow-free on 21 April, their albedo decreased abruptly, while the decrease in albedo on the plateau forests was more prolonged (Figure 6(g)). The snow-free wetlands were also able to contribute energy for snowmelt in adjacent forests through local advection (e.g., Granger et al., 2002). The dense forest plateau snow cover received the greatest incoming longwave radiation of all the sites, owing to the greater amount of canopy surface area available to emit longwave radiation. Incoming longwave radiation in the dense forest increased relative to other sites as the melt season progressed and the

canopy temperature rose. Outgoing longwave radiation measured over the snow surface was similar among all sites indicating relatively homogenous snow surface temperatures of  $\sim 0^{\circ}\text{C}$ . The contribution to melt from longwave radiation remained secondary to shortwave radiation throughout the melt period.

Helbig et al. (2016a) projected a net regional cooling effect over a hypothetical continuous wetland terrain partly because of increased late winter albedo resulting from the loss of forest cover. The results presented here agree with their projection of an increased albedo, and we suggest that the cooling predicted by Helbig et al. (2016a) may be partly

offset by earlier and more rapid snowmelt in wetlands than in the surrounding forested plateaus. Wetland expansion on the landscape may therefore result in earlier hydrograph peaks during the spring freshet.

## 5.4 | Permafrost thaw-induced hydrological change

Despite statistically significant ( $p < 0.01$ ) differences between end-of-winter SWE in forested plateaus and wetlands, the magnitude of

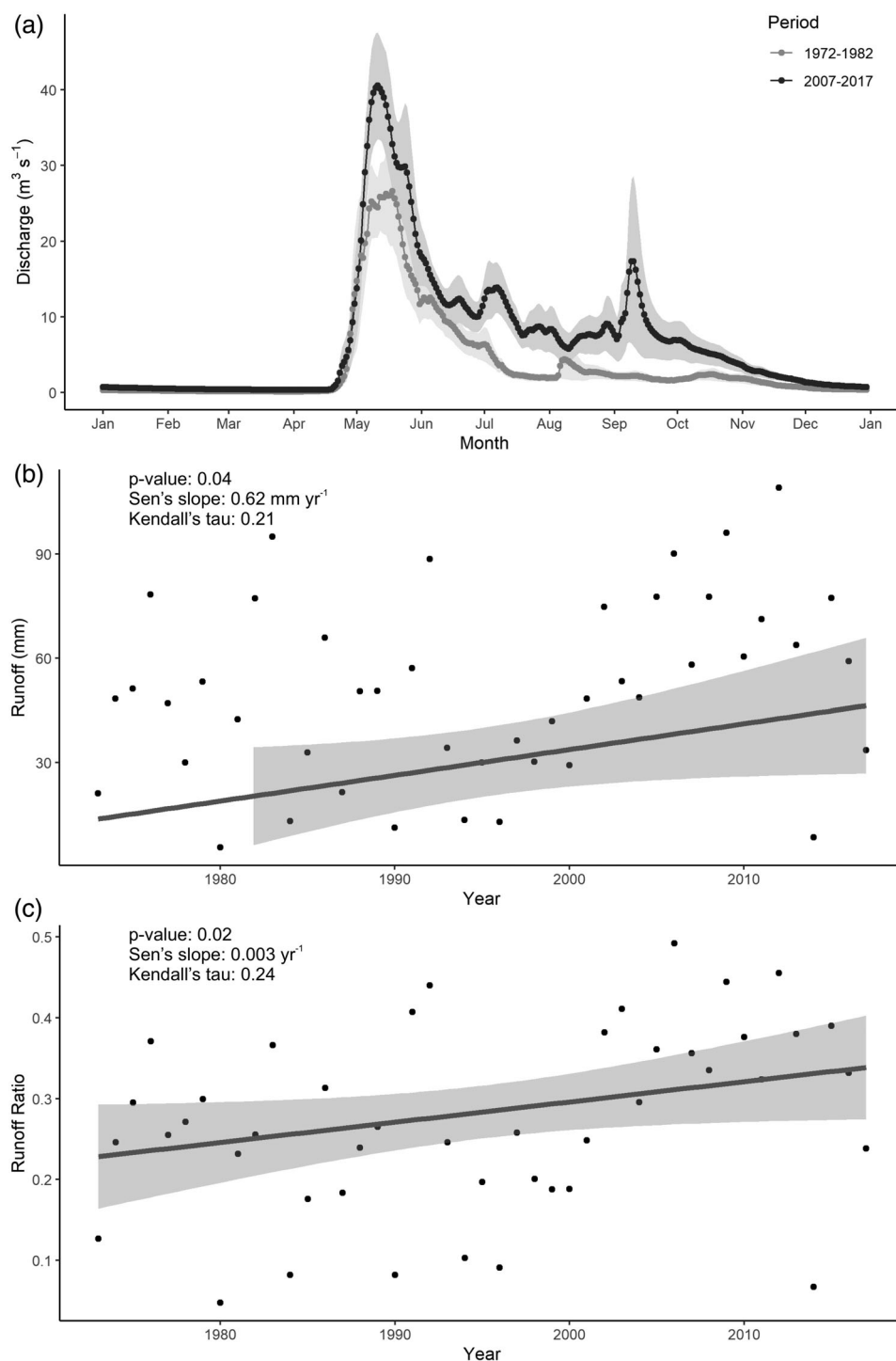


**FIGURE 8** (a) Composite hydrographs for 11 year periods of 1972–1982 and 2005–2015 for the Jean Marie River; (b) the snowmelt runoff (i.e., April and May runoff) portion of the annual hydrograph; and (c) runoff ratios for the Jean Marie River for the years 1977 to 2010 trends are statistically significant at  $p < 0.05$

these differences is too low to result in an appreciable change in the area-weighted average basin SWE resulting from the transition of forest to wetland. The reduction in area-weighted SWE as a result of the permafrost thaw induced conversion of forest to wetland is far less than the inter-annual variability of SWE. Furthermore, the extreme case of a conversion of all remaining forested plateaus to treeless wetlands would decrease the area-weighted SWE by only 5.1% from 1970.

Permafrost thaw-induced changes to wetland storage and routing processes (Connon et al., 2015; Connon et al., 2018) coincided with extended, multi-year periods of increasing annual basin runoff throughout the study region (Chasmer & Hopkinson, 2016; St Jacques & Sauchyn, 2009). Connon et al. (2014) reported that between 1977 and 2010, the portion of a 6 km<sup>2</sup> area that is hydrologically-connected to channel fens and therefore to the basin drainage outlet, had increased from approximately 31%–42% as a result of permafrost thaw. This increase in hydrological connectivity suggests fundamental changes to the routing and storage of water within basins underlain by rapidly thawing, discontinuous permafrost.

A change in the hydrological functioning of the Jean-Marie River is evident when comparing its hydrograph associated with its land cover in 1977 with that associated with its permafrost degraded land cover in 2010. This is demonstrated by comparing composite hydrographs of two 11-year periods centred on 1977 (1972–1982) and 2010 (2005–2015). There is a distinct increase in both the magnitude and the duration of the freshet peak between the two periods (Figure 8(a)). Furthermore, there is a significant ( $p < 0.05$ ) increase of 0.6 mm year<sup>-1</sup> in snowmelt (April and May) runoff, as well as snowmelt runoff ratios at Jean-Marie River over the period of record (1972–2018) (Figure 8(b), (c)). The absence of a statistically significant change in SWE at Fort Simpson between 1970 and 2018 suggests that the increase in snowmelt arose from a change in runoff and storage processes. A plausible explanation for this increased runoff efficiency is that it results from the permafrost thaw-induced increase in hydrological connectivity, either from more hydrologically integrated peat plateau-wetland complexes (Connon et al., 2014), and/or losses of suprapermfrost groundwater storage (Chasmer & Hopkinson, 2016), which may be slowly released through taliks or perennially thawed zones (Walvoord et al., 2019) and portions of the basin previously impounded by permafrost (Haynes et al., 2018). The resulting increased fraction of the areal SWE that can contribute to runoff, as well as the more rapid melt in a wetland-dominated landscape, may therefore be a primary factor driving the increase in basin runoff from Jean-Marie River, Scotty Creek, and elsewhere in the region. This increase in SWE available for runoff due to the permafrost thaw-induced changes in hydrological connectivity and melt rates greatly outweighs the negligible decrease in the area-weighted average basin SWE resulting from the transition of forests to wetlands. Given the typically high runoff ratios of the snowmelt runoff period in the study region, changes to the routing of surface and subsurface flows can have a discernible impact on the basin hydrograph.

## 6 | CONCLUSIONS

Recent work in the southern fringe of the discontinuous permafrost zone in the Dehcho region of northwestern Canada has demonstrated that the relative proportions of peat plateau forests (permafrost features) and open wetlands (permafrost-free features) are changing due to climate warming. We found small, but statistically significant differences ( $p < 0.01$ ) in end-of-winter SWE between plateau forests and wetlands, but found that this difference is not large enough to cause an appreciable change in area-weighted SWE across the basin. However, with continued wetland expansion, it is reasonable to expect that the annual snowmelt event will become more rapid (i.e., wetland-like), resulting in earlier and longer snow-free conditions, allowing greater cumulative energy available for ground thaw and other processes. The amount of SWE available for basin runoff may also increase, as has been documented by a statistically significant increasing trend ( $p < 0.05$ ) of snowmelt runoff in the Jean Marie River basin, despite no statistically significant trend ( $p > 0.05$ ) of changing SWE availability in the region.

## ACKNOWLEDGEMENTS

The authors wish to thank the offices of the Liidlii Kue First Nation, the Jean-Marie River First Nation, and the Dehcho First Nations for their support of both the Scotty Creek Research Station and this project. We also gratefully acknowledge ArcticNet for their support of the Dehcho Collaborative on Permafrost, the Natural Sciences Engineering Research Council (NSERC), the Northern Studies Training Program (NSTP), the Garfield Weston Foundation, and the Cold Regions Research Centre. We also wish to thank Michael Braverman, Olivia Carpino, Dr. Elise Devoie, Jessica Hanisch, Alex MacLean, Jared Simpson, Lindsay Stone, and Nick Wilson for their assistance throughout this study. We would like to thank the Editor and an anonymous reviewer for greatly improving the quality of this manuscript.

## DATA AVAILABILITY STATEMENT

The data and R scripts used in this manuscript are available by contacting the corresponding author.

## ORCID

Ryan F. Connon  <https://orcid.org/0000-0002-2420-3609>

## REFERENCES

- Aylesworth, J. M., & Kettles, I. M. (2000). Distribution of peatlands. *Natural Resources Canada, Geological Survey of Canada Bulletin*, 547, 49–55.
- Baltzer, J. L., Veness, T., Chasmer, L. E., Sniderhan, A. E., & Quinton, W. L. (2014). Forests on thawing permafrost: Fragmentation, edge effects, and net forest loss. *Global Change Biology*, 20(3), 824–834. <https://doi.org/10.1111/gcb.12349>
- Box, J. E., Colgan, W. T., Christensen, T. R., Schmidt, N. M., Lund, M., Parmentier, F.-J. W., Brown, R., Bhatt, U. S., Euskirchen, E. S., Romanovsky, V. E., Walsh, J. E., Overland, J. E., Wang, M., Corell, R. W., Meier, W. N., Wouters, B., Mernild, S., Mård, J., Pawlak, J., & Olsen, M. S. (2019). Key indicators of Arctic climate change: 1971–2017. *Environmental Research Letters*, 14, 045010. <https://doi.org/10.1088/1748-9326/aafc1b>



- Carpino, O. A., Berg, A. A., Quinton, W. L., & Adams, J. R. (2018). Climate change and permafrost thaw-induced boreal forest loss in northwestern Canada. *Environmental Research Letters*, 13, 084018. <https://doi.org/10.1088/1748-9326/aad74e>
- Cartwright, K. A., Hopkinson, C., Kienzie, S., & Rood, S. B. (2020). Evaluation of temporal consistency of snow depth drivers of a Rocky Mountain watershed in southern Alberta. *Hydrological Processes*, 34, 4996–5012. <https://doi.org/10.1002/hyp.13920>
- Chasmer, L., & Hopkinson, C. (2016). Threshold loss of discontinuous permafrost and landscape evolution. *Global Change Biology*, 23, 2672–2686. <https://doi.org/10.1111/gcb.13537>
- Chasmer, L., Hopkinson, C., Veness, T., Quinton, W., & Baltzer, J. (2014). A decision-tree classification for low-lying complex land cover types within the zone of discontinuous permafrost. *Remote Sensing of Environment*, 143, 73–84. <https://doi.org/10.1016/j.rse.2013.12.016>
- Chasmer, L., Quinton, W. L., Hopkinson, C., Petrone, R., & Whittington, P. (2011). Vegetation canopy and radiation controls on permafrost plateau evolution within the discontinuous permafrost zone, Northwest Territories, Canada. *Permafrost and Periglacial Processes*, 22, 199–213. <https://doi.org/10.1002/ppp.724>
- Connon, R., Devoie, É., Hayashi, M., Veness, T., & Quinton, W. (2018). The influence of shallow taliks on permafrost thaw and active layer dynamics in subarctic Canada. *Journal of Geophysical Research: Earth Surface*, 123, 1–17. <https://doi.org/10.1002/2017JF004469>
- Connon, R. F., Quinton, W. L., Craig, J. R., Hanisch, J., & Sonnentag, O. (2015). The hydrology of interconnected bog complexes in discontinuous permafrost terrains. *Hydrological Processes*, 29(18), 3831–3847. <https://doi.org/10.1002/hyp.10604>
- Connon, R. F., Quinton, W. L., Craig, J. R., & Hayashi, M. (2014). Changing hydrologic connectivity due to permafrost thaw in the lower Liard River valley, NWT, Canada. *Hydrological Processes*, 28(14), 4163–4178. <https://doi.org/10.1002/hyp.10206>
- Davis, R. E., Hardy, J. P., Ni, W., Woodcock, C., McKenzie, J. C., Jordan, R., & Li, X. (1996). Variation of snow cover ablation in the boreal forest: A sensitivity study on the effects of conifer canopy. *Journal of Geophysical Research: Atmospheres*, 102(D24), 389–395. <https://doi.org/10.1029/97JD01335>
- Devoie, É. G., Craig, J. R., Connon, R. F., & Quinton, W. L. (2019). Taliks: A tipping point in discontinuous permafrost degradation in peatlands. *Water Resources Research*, 55, 1–20.
- Disher, B., Connon, R. F., Haynes, K. M., Hopkinson, C., & Quinton, W. L. (2021). The hydrology of treed wetlands in thawing discontinuous permafrost regions. *Ecohydrology*, 14, 1–15. <https://doi.org/10.1002/eco.2296>
- Dixon, D., & Boon, S. (2012). Comparison of the SnowHydro snow sampler with existing snow tube designs. *Hydrological Processes*, 26(17), 2555–2562. <https://doi.org/10.1002/hyp.9317>
- Farnes, P. E., Peterson, N. R., Goodison, B. E., & Richards, R. P. (1982). *Met-rication of manual snow sampling equipment, paper presented at 50<sup>th</sup> Western snow conference* (pp. 120–132). Western Snow Conference.
- Fischer, A. P. (2011). The measurement factors in estimating snowfall derived from snow cover surfaces using acoustic snow depth sensors. *Journal of Applied Meteorology and Climatology*, 50(3), 681–699. <https://doi.org/10.1175/2010JAMC2408.1>
- Garon-Labrecque, M. È., Léveillé-Bourret, É., Higgins, K., & Sonnentag, O. (2016). Additions to the boreal flora of the Northwest Territories with a preliminary vascular flora of Scotty Creek. *The Canadian Field-Naturalist*, 129(4), 349–367. <https://doi.org/10.22621/cfn.v129i4.1757>
- Golding, D. L., & Swanson, R. H. (1986). Snow distribution patterns in clearings and adjacent forest. *Water Resources Research*, 22(13), 1931–1940. <https://doi.org/10.1029/WR022i013p01931>
- Goodison, B. E., Louie, P. T., & Yang, D. (1998). WMO solid precipitation measurement intercomparison – Final report. *Instruments and observing methods report no. 67 WMO/TD no. 872*, Geneva: World Meteorological Organization.
- Goodrich, L. E. (1982). The influence of snow cover on the ground thermal regime. *Canadian Geotechnical Journal*, 19, 421–432. <https://doi.org/10.1139/t82-047>
- Granger, R. J., Pomeroy, J. W., & Parviainen, J. (2002). Boundary-layer integration approach to advection of sensible heat to a patchy snow cover. *Hydrological Processes*, 16(18), 3559–3569. <https://doi.org/10.1002/hyp.1227>
- Gray, D. M., Toth, B., Zhao, L., Pomeroy, J. W., & Granger, R. J. (2001). Estimating areal snowmelt infiltration into frozen soils. *Hydrological Processes*, 15(16), 3095–3111. <https://doi.org/10.1002/hyp.320>
- Hamlin, L., Pietroniro, A., Prowse, T., Soulis, R., & Kouwen, N. (1998). Application of indexed snowmelt algorithms in a northern wetland regime. *Hydrological Processes*, 12(10–11), 1641–1657. [https://doi.org/10.1002/\(SICI\)1099-1085\(199808/09\)12:10/11<1641::AID-HYP686>3.0.CO;2-W](https://doi.org/10.1002/(SICI)1099-1085(199808/09)12:10/11<1641::AID-HYP686>3.0.CO;2-W)
- Hayashi, M., Quinton, W. L., Pietroniro, A., & Gibson, J. J. (2004). Hydrological functions of interconnected wetlands in a discontinuous permafrost basin indicated by isotopic and chemical signatures. *Journal of Hydrology*, 296, 81–97. <https://doi.org/10.1016/j.jhydrol.2004.03.020>
- Haynes, K. M., Connon, R. F., & Quinton, W. L. (2018). Permafrost thaw induced drying of wetlands at Scotty Creek, NWT, Canada. *Environmental Research Letters*, 13, 114001. <https://doi.org/10.1088/1748-9326/aae46c>
- Haynes, K. M., Connon, R. F., & Quinton, W. L. (2019). Hydrometeorological measurements in peatland-dominated, discontinuous permafrost at Scotty Creek, Northwest Territories, Canada. *Geoscience Data Journal*, 6, 85–96. <https://doi.org/10.5683/SP/OQDRJG>
- Helbig, M., Pappas, C., & Sonnentag, O. (2016). Permafrost thaw and wildfire: Equally important drivers of boreal tree cover changes in the Taiga Plains, Canada. *Geophysical Research Letters*, 43, 1598–1606. <https://doi.org/10.1002/2015GL067193>
- Helbig, M., Wischewski, K., Kijun, N., Chasmer, L. E., Quinton, W. L., Detto, M., & Sonnentag, O. (2016). Regional atmospheric cooling and wetting effect of permafrost thaw-induced boreal forest loss. *Global Change Biology*, 22, 4048–4066. <https://doi.org/10.1111/gcb.13348>
- Helsel, D. R., & Hirsch, R. M. (2002). Statistical methods in water resources (chapter A3). In *Book 4, hydrologic analysis and interpretation* (p. 510). United States Geological Survey.
- Hiemstra, C. A., Liston, G. E., & Reiners, W. A. (2002). Snow redistribution by wind and interactions with vegetation at upper treeline in the medicine Bow Mountains, Wyoming, USA. *Arctic, Antarctic and Alpine Research*, 34, 262–273. <https://doi.org/10.1080/15230430.2002.12003493>
- Hinzman, L. D., Bettez, N. D., Bolton, W. R., Chapin, F. S., Dyrgerov, M. B., Fastie, C. L., & Jensen, A. M. (2005). Evidence and implications of recent climate change in northern Alaska and other Arctic regions. *Climatic Change*, 72(3), 251–298. <https://doi.org/10.1007/s10584-005-5352-2>
- Jorgenson, M. T., & Osterkamp, T. E. (2005). Response of boreal ecosystems to varying modes of permafrost degradation. *Canadian Journal of Forestry Research*, 35, 2100–2111. <https://doi.org/10.1139/X05-153>
- Jorgenson, M. T., Racine, C. H., Walters, J. C., & Osterkamp, T. E. (2001). Permafrost degradation and ecological changes associated with a warming climate in Central Alaska. *Climatic Change*, 48, 551–579. <https://doi.org/10.1023/A:1005667424292>
- Kendall, M. (1975). *Rank correlation methods*. Griffin.
- Kinar, N. J., & Pomeroy, J. W. (2015). Measurement of the physical properties of the snowpack. *Reviews of Geophysics*, 53, 1–64. <https://doi.org/10.1002/2015RG000481>
- Kruskal, W. H., & Wallis, W. A. (1952). Use of ranks in one-criterion variance analysis. *Journal of the American Statistical Association*, 47(260), 583–621.
- Kurylyk, B. L., Hayashi, M., Quinton, W. L., McKenzie, J. M., & Voss, C. I. (2016). Influence of vertical and lateral heat transfer on permafrost thaw, peatland landscape transition, and groundwater flow. *Water Resources Research*, 52, 1286–1305. <https://doi.org/10.1002/2015WR018057>

- Kwong, Y. J., & Gan, T. Y. (1994). Northward migration of permafrost along the Mackenzie highway and climatic warming. *Climatic Change*, 26(4), 399–419. <https://doi.org/10.1007/BF01094404>
- Maxwell, J., & St Clair, S. (2019). Snowpack properties vary in response to burn severity gradients in montane forests. *Environmental Research Letters*, 14, 124094. <https://doi.org/10.1088/1748-9326/ab5de8>
- McClymont, A. F., Hayashi, M., Bentley, L., & Christensen, B. (2013). Geophysical imaging and thermal modeling of subsurface morphology and thaw evolution of discontinuous permafrost. *Journal of Geophysical Research: Earth Surface*, 118, 1–12. <https://doi.org/10.1002/jgrf.20114>
- Mekis, É., & Brown, R. (2010). Derivation of an adjustment factor map for the estimation of the water equivalent of snowfall from ruler measurements Canada. *Atmosphere-Ocean*, 48(4), 284–293. <https://doi.org/10.3137/AO1104.2010>
- Mekis, É., Donaldson, N., Reid, J., Zucconi, A., Hoover, J., Li, Q., & Melo, S. (2018). An overview of surface-based precipitation observations at environment and climate change Canada. *Atmosphere-Ocean*, 56(2), 71–95. <https://doi.org/10.1080/07055900.2018.1433627>
- Mekis, É., & Hopkinson, R. (2004). Derivation of an improved snow water equivalent adjustment factor map for application on snowfall ruler measurements in Canada. In *Proceedings of the 14th Conference on Applied Climatology*. American Meteorological Society, Seattle, WA.
- Mekis, É., & Vincent, L. A. (2011). An overview of the second generation adjusted daily precipitation dataset for trend analysis in Canada. *Atmosphere-Ocean*, 49(2), 163–177. <https://doi.org/10.1080/07055900.2011.583910>
- Murray, C. D., & Buttle, J. M. (2003). Impacts of clearcut harvesting on snow accumulation and melt in a northern hardwood forest. *Journal of Hydrology*, 271, 197–212. [https://doi.org/10.1016/S0022-1694\(02\)000352-9](https://doi.org/10.1016/S0022-1694(02)000352-9)
- National Wetlands Working Work (NWWG). 1988. *Wetlands of Canada*. Ecological land classification series, No. 24. Sustainable Development Branch, Environment Canada/Polyscience Publications Inc. Ottawa, Ontario.
- Pachauri, R.K., & Reisinger, A. (Eds.). (2007). Climate change 2007 synthesis report: Summary for policymakers. IPCC Secretariat.
- Pomeroy, J.W., & Schmidt, R.A. (1993). The use of fractal geometry in modeling intercepted snow accumulation and sublimation. In *Proceedings of the eastern snow conference*, 50, 1–10.
- Pulliainen, J., Aurela, M., Laurila, T., Aalto, T., Takala, M., Salminen, M., Kulmala, M., Barr, A., Heimann, M., Lindroth, A., Laaksonen, A., Derksen, C., Mäkelä, A., Markkanen, T., Lemmetyinen, J., Susiluoto, J., Dengel, S., Mammarella, I., Tuovinen, J. P., & Vesala, T. (2017). Early snowmelt significantly enhances boreal springtime carbon uptake. *Proceedings of the National Academy of Sciences*, 114(42), 11081–11086. <https://doi.org/10.1073/pnas.1707889114>
- Putkonen, J., Grenfell, T. C., Rennert, K., Bitz, C., Jacobson, P., & Russell, D. (2009). Rain on snow: Little understood killer in the north. *Eos, Transactions American Geophysical Union*, 90(26), 221–222. <https://doi.org/10.1029/2009EO260002>
- Quinton, W. L., Hayashi, M., & Chasmer, L. E. (2009). Peatland hydrology of discontinuous permafrost in the Northwest Territories: Overview and synthesis. *Canadian Water Resources Journal*, 34(4), 311–328. <https://doi.org/10.4296/cwrj3404311>
- Quinton, W. L., Hayashi, M., & Chasmer, L. E. (2011). Permafrost-thaw-induced land-cover change in the Canadian subarctic: Implications for water resources. *Hydrological Processes*, 25(1), 152–158. <https://doi.org/10.1002/hyp.7894>
- Quinton, W. L., Hayashi, M., & Pietroniro, A. (2003). Connectivity and storage functions of channel fens and flat bogs in northern basins. *Hydrological Processes*, 17(18), 3665–3684. <https://doi.org/10.1002/hyp.1369>
- R Core Team. (2013). *R: A language and environment for statistical computing*. R Foundation for Statistical Computing.
- Robinson, S. D., & Moore, T. R. (2000). The influence of permafrost and fire upon carbon accumulation in high boreal peatlands, Northwest Territories, Canada. *Arctic, Antarctic, and Alpine Research*, 32(2), 155–166. <https://doi.org/10.1080/15230430.2000.12003351>
- Roulet, N. T., & Woo, M. K. (1986). Hydrology of a wetland in the continuous permafrost region. *Journal of Hydrology*, 89(1–2), 73–91. [https://doi.org/10.1016/0022-1694\(86\)90144-7](https://doi.org/10.1016/0022-1694(86)90144-7)
- Semmens, K. A., Ramage, J., Bartsh, A., & Liston, G. E. (2013). Early snow-melt events: Detection, distribution, and significance in a major sub-arctic watershed. *Environmental Research Letters*, 8, 014020. <https://doi.org/10.1088/1748-9326/8/1/014020>
- Sicart, J. E., Essery, R. L., Pomeroy, J. W., Hardy, J., Link, T., & Marks, D. (2004). A sensitivity study of daytime net radiation during snowmelt to forest canopy and atmospheric conditions. *Journal of Hydrometeorology*, 5(5), 774–784. [https://doi.org/10.1175/1525-7541\(2004\)005<0774:ASSODN>2.0.CO;2](https://doi.org/10.1175/1525-7541(2004)005<0774:ASSODN>2.0.CO;2)
- St Jacques, J. M., & Sauchyn, D. J. (2009). Increasing winter baseflow and mean annual streamflow from possible permafrost thawing in the Northwest Territories, Canada. *Geophysical Research Letters*, 36(1), 1–6. <https://doi.org/10.1029/2008GL035822>
- Storck, P., Lettenmaier, D. P., & Bolton, S. M. (2002). Measurement of snow interception and canopy effects on snow accumulation and melt in mountainous maritime climate, Oregon, United States. *Water Resources Research*, 38(11), 1223–1238. <https://doi.org/10.1029/2002WR001281>
- Thie, J. (1974). Distribution and thawing of permafrost in the southern part of the discontinuous permafrost zone in Manitoba. *Arctic Journal of the Arctic Institute of North America*, 27(3), 189–200. <https://doi.org/10.14430/arctic2873>
- Varhola, A., Coops, N., Bater, C. W., Teti, P., Boon, S., & Weiler, M. (2010). The influence of ground- and lidar-derived forest structure metrics on snow accumulation and ablation in disturbed forests. *Canadian Journal of Forest Research*, 40(4), 812–821. <https://doi.org/10.1139/X10-008>
- Vincent, L. A., Zhang, X., Brown, R. D., Feng, Y., Mekis, E., Milewska, E. J., Wan, H., & Wang, X. L. (2015). Observed trends in Canada's climate and influence of low-frequency variability modes. *Journal of Climate*, 28(11), 4545–4560. <https://doi.org/10.1175/JCLI-D-14-00697.1>
- Walvoord, M. A., Voss, C. I., Ebel, B. A., & Minsley, B. J. (2019). Development of perennial thaw zones in boreal hillslopes enhances potential mobilization of permafrost carbon. *Environmental Research Letters*, 14, 015003. <https://doi.org/10.1088/1748-9326/aaf0cc>
- Webster, C., Rutter, N., Zahnner, F., & Jonas, T. (2016). Measurement of incoming radiation below forest canopies: A comparison of different radiometer configurations. *Journal of Hydrometeorology*, 17(3), 853–864. <https://doi.org/10.1175/JHM-D-0125.1>
- Winkler, R. D., Spittlehouse, D. L., & Golding, D. L. (2005). Measured differences in snow accumulation and melt among clearcut, juvenile, and mature forests in southern British Columbia. *Hydrological Processes*, 19(1), 51–62. <https://doi.org/10.1002/hyp.5757>
- Zoltai, S. C. (1993). Cyclic development of permafrost in the peatlands of northwestern Alberta, Canada. *Arctic and Alpine Research*, 3, 240–246. <https://doi.org/10.2307/1551820>

**How to cite this article:** Connon, R. F., Chasmer, L., Haughton, E., Helbig, M., Hopkinson, C., Sonnentag, O., & Quinton, W. L. (2021). The implications of permafrost thaw and land cover change on snow water equivalent accumulation, melt and runoff in discontinuous permafrost peatlands. *Hydrological Processes*, 35(9), e14363. <https://doi.org/10.1002/hyp.14363>